

InSAR Time Series Analysis of Crustal Deformation associated with the August 2014 M6 Napa Valley Earthquake in California

Ayanna Reed

¹The City University of New York at Lehman College, Dept. of Earth, Environmental & Geospatial Science, 250 Bedford Park Blvd West, Bronx, NY 10468

Abstract

One year following the August 2014 magnitude 6 South Napa Valley earthquake in California, we used persistent scatterer radar interferometry (PSInSAR) to generate a time series of 56 interferograms via the short baseline subset approach (SBAS). The interferograms were used to detect evidence of crustal deformation in the South Napa region prior to the event. Detection of preseismic deformation was essential to our objective of testing the feasibility of creating a consistent and reliable early warning system via space based methods. Raw (level 1.0) ALOS PALSAR satellite data (22 images spanning 2007-2011), initially acquired by JAXA (Japan Aerospace Exploration Agency) and secondly stored in the data archives by the Alaska Satellite Facility, was used for this study. For SAR processing, we used Remote Sensing Software Graz from the Joanneum Research Institute.

In this time series, no significant deformation was detected prior to the event. We conclude that it is beneficial to our future research to observe regions of actively deforming faults. We find that in the absence of extended periods of low seismic activity, such as in the 25 years of low seismic activity in South Napa, we are more likely to detect preseismic deformation.

Keywords: Persistent scatterer, InSAR, preseismic deformation, short baseline subset approach (SBAS)

Introduction

Earthquakes are one of the deadliest natural hazards in the state of California. Until 2014, California was ranked second behind Alaska as the state with the most recorded earthquakes until it was surpassed by Oklahoma in 2015 (USGS Website Source: http://earthquake.usgs.gov/learn/topics/megaqk_facts_fantasy.php). In August 2014, a magnitude 6.0 strike slip earthquake struck the South Napa Valley region in California. It was the first significant event to occur in Napa Valley in 25 years. This extended period of low seismic activity is known as a “seismic shadow” (USGS). The South Napa Earthquake had a shallow depth of 11.2 km and occurred 9 km southwest of Napa, within the West Napa Fault System (between the Hayward-Rodgers Creek Fault System to the west of the epicenter and the Concord-Green Valley Fault System to the east of the epicenter) (USGS).

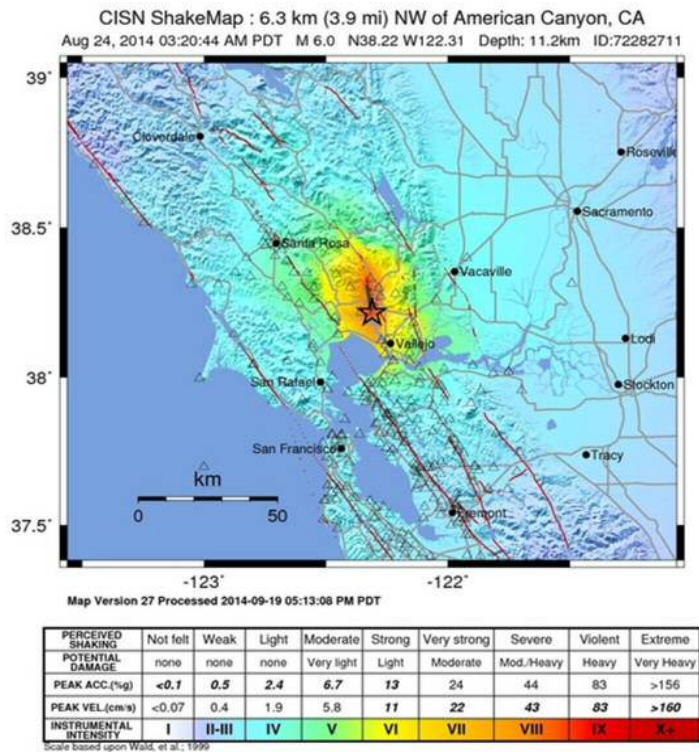


Figure 1. USGS ShakeMap of the 2014 M6 South Napa Earthquake

Detection of pre-seismic deformation was essential to our objective of testing the feasibility of creating a consistent and reliable early warning system via space based methods. Monitoring ground displacement associated with seismic activity is important for establishing earthquake warning systems and strengthening mitigation and evacuation strategies. But, this is difficult given that earthquakes cannot be precisely predicted. Measuring ground displacement with accuracy is essential to developing models that analyze the strain and stress of slow slip events. Integrated approaches to analyzing crustal deformation associated with seismicity include using space and ground observations. Hence, Persistent Interferometric Synthetic Aperture Radar (PSInSAR) was used to generate a pre-seismic time series analysis to assess the crustal deformation associated with the August 2014 M6 South Napa Valley earthquake in California. In this study, we applied Persistent Scatter InSAR & the short baseline subset approach (SBAS), a space-based technique of Interferometric Synthetic Aperture Radar (InSAR), to detect and measure the surface displacement associated with the event at centimeter to millimeter level accuracy. We aimed to detect any anomalies of surface displacement prior to the event that may have served as indicators of the impending rupture via the time series data set of interferograms we generated. In Figure 1, the United States Geological Survey produced a shake map of the event to show the distribution of the intensity of the earthquake throughout the region.

Data

For this project, initially the software of Cornell University named Repeat Orbit Interferometry Software Package (ROI_PAC) was to be used. But, there were problems with generating the required digital elevation model to initiate the synthetic aperture radar (SAR) processing. Therefore, the next option was to use the radar interferometry software of the University of California at San Diego named Generic Mapping Tools (GMTSAR) by David Sandwell et al. (Sandwell et al. 2011). But with this software, the issue presented was that the persistent scatter algorithm was not compatible with the Windows operating system we were using for this project. Therefore, the last option for software was the Remote Sensing Software Graz by the Joanneum Research Institute. This software includes the Persistent Scatter algorithm to process a stack of SAR images. Also, we used a 30 meter SRTM 1 digital elevation model over the United States via the DEM Generator of the GMTSAR website. Furthermore, Cygwin was the UNIX operating system environment used to process the raw data and produce the interferograms.

The satellite data used for this project was acquired by the ALOS PALSAR (Advanced Land Observation Satellite & the Phased Array Type L Band Synthetic Aperture Radar Sensor) of the Japan Aerospace Exploration Agency (JAXA). The images are stored in the SAR archives of the Alaska Satellite Facility. In figure 2 below are the 22 images used for this project and their characteristics. All images were acquired over the South Napa Valley Region in California.

| ID | Orbit | Acquisition Date | Δ Time | Single Polarization | Dual Polarization | Baseline Perp. (m) |
|----|-------|------------------|---------------|---------------------|-------------------|--------------------|
| 1 | 7136 | 28-May-07 | 46 | X | | 0 |
| 2 | 7807 | 13-Jul-07 | 46 | | X | 686.2 |
| 3 | 8478 | 28-Aug-07 | 46 | | X | 903 |
| 4 | 9149 | 13-Oct-07 | 46 | | X | 1392.2 |
| 5 | 9820 | 28-Nov-07 | 46 | X | | 1221.2 |
| 6 | 10491 | 13-Jan-08 | 46 | X | | 1907.4 |
| 7 | 11162 | 28-Feb-08 | 46 | X | | 2486 |
| 8 | 11833 | 14-Apr-08 | 46 | X | | 2871.3 |
| 9 | 12504 | 30-May-08 | 46 | | X | 2679.4 |
| 10 | 13175 | 15-Jul-08 | 46 | | X | -372.2 |
| 11 | 15188 | 30-Nov-08 | 138 | X | | -1706.7 |
| 12 | 15859 | 15-Jan-09 | 46 | X | | -1178.8 |
| 13 | 16530 | 2-Mar-09 | 46 | X | | -932.1 |
| 14 | 17872 | 2-Jun-09 | 92 | X | | -821.2 |
| 15 | 18543 | 18-Jul-09 | 46 | | X | -339.2 |
| 16 | 19885 | 18-Oct-09 | 92 | | X | 373.2 |
| 17 | 21227 | 18-Jan-10 | 92 | X | | 833.1 |
| 18 | 22569 | 20-Apr-10 | 92 | X | | 1584.3 |
| 19 | 23240 | 5-Jun-10 | 46 | | X | 1821.9 |
| 20 | 23911 | 21-Jul-10 | 46 | | X | 1876.9 |
| 21 | 25924 | 6-Dec-10 | 138 | | X | 2399.2 |
| 22 | 27266 | 8-Mar-11 | 92 | X | | 3373.7 |

Figure 2: Raw Level 1.0 images acquired over the South Napa Valley region used for processing

The wavelength of the L Band on the PALSAR sensor is 23 centimeters (JAXA). The L Band of the PALSAR sensor has the longest wavelength of the radar waves and allows for better penetration of the emitted signal through vegetation, the nighttime, rain, clouds and all weather (JAXA). The repeat cycle for the ALOS PALSAR satellite is 46 days.

All raw level 1.0 data was acquired on ascending orbits via single polarization (HH-horizontally transmitted and horizontally received) and double polarization mode (HH and VV-vertically transmitted and vertically received) modes. The image dates span from 2007 to 2011 and the ideal critical baseline for analysis is <1000m. However, we had difficulty acquiring images with a consistently ideal critical baseline with ALOS PALSAR. Despite this challenge, we were not hindered from using the persistent scatter method to analyze a time series data detecting crustal deformation.

Radar Interferometry

Interferometric Synthetic Aperture Radar (InSAR) involves the process of sending radar signals to a particular position on the earth’s surface and detecting the changes in elevation (uplift, subsidence, or horizontal movement) of this position on the ground. InSAR requires two or more images acquired over the same area but taken at different times. InSAR detects changes in elevation between the time the first image (or the Master Image) and second image (or the Slave Image) was acquired (Lu, ASF, 2006). An interferogram image is the result of InSAR processing and thus displays information about the phase change (also known as range change or range distance difference) (USGS and ASF) which is “...determined primarily by the distance between the satellite antenna and the ground targets” (ESA). Hence, an interferogram is the result of the change in phase.

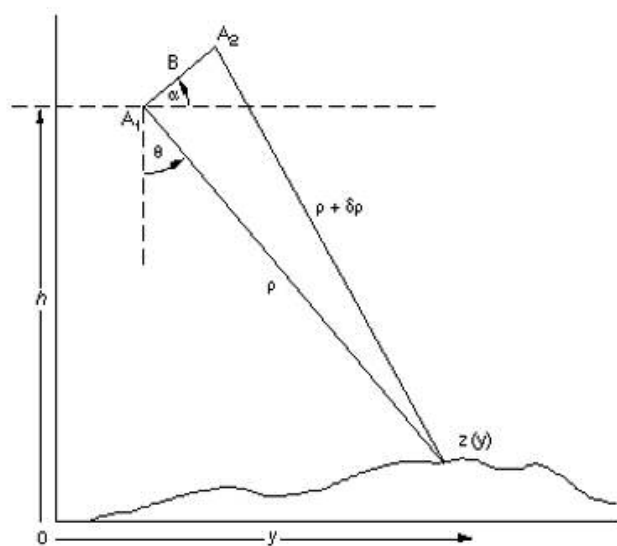


(Image and variables source: European Space Agency)

Where:

A_1 is the 1st pass or 1st satellite at height h above surface

A_2 is the 2nd pass or 2nd satellite at height h above surface

ρ is the slant range

$\rho + \rho\delta$ is the distance between A_2 and the ground point

B is the baseline or distance between the SAR satellite orbits for the first and second observations

Figure 3: Diagram of InSAR

As of yet, there are no reliable or consistent methods of predicting earthquakes. Several precursory anomalies such as increases in Chlorophyll-a concentration, land surface temperature, and near-ground air temperature have been investigated. However, many Geophysicists remain skeptical about the nature of several of these anomalies and if their occurrence is associated with seismic activity. Radar Interferometry is a science that aims to detect seismic precursors such as crustal deformation. This is also bringing Geophysicists closer to finding a reliable technique and technology to decipher the nature of earthquakes or even hopefully to predict them. Thus, InSAR is one of several techniques at the forefront of modeling surface displacements induced by seismicity.

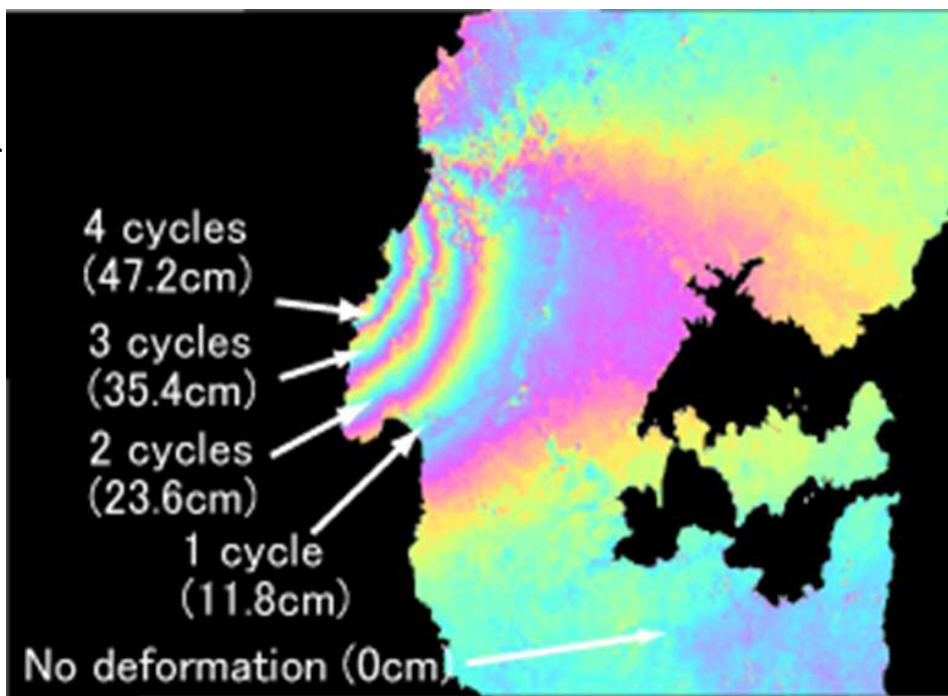
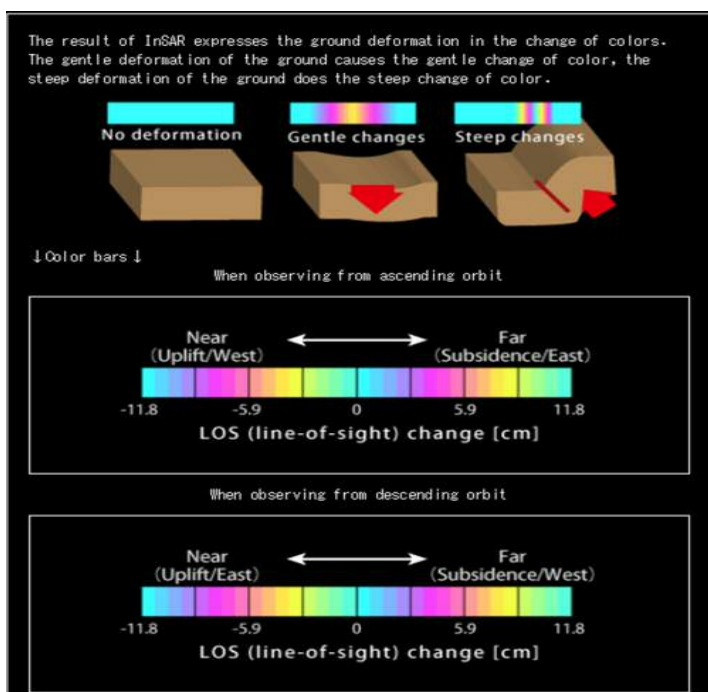


Figure 4a: Fringes of an Interferogram (JAXA)



←Phase change is due to a change in range (deformation) (JAXA). Therefore surface deformation is detected within the line of sight (LOS).

Figure 4b: How to read an interferogram (JAXA)

Methodology

Figure 5 represents the basic interferometry processing chain (Chelbi et al. 2011) that requires a master image (earlier date) and a slave image (later date) to initiate the process. Once these two images are acquired, they must be co-registered on a pixel by pixel basis so that the slave image aligns with the master image (Chelbi et al. 2011). After coregistration, the following step is the filtering of the azimuth, range, or phase. Azimuth filtering involves the filtering of a single look complex stack of master and slave images in the azimuth direction, or the along-track, which is parallel to the satellite path direction (ESA).

Range filtering involves the filtering of a single look complex stack of master and slave images in the range direction, or the across-track, which is perpendicular to the satellite path direction (ESA). Azimuth and range filtering require a co-registered stack of master and slave images to begin the filtering process. Thirdly, phase filtering requires an input of interferograms to begin this process. Filtering of phase: 1) reduces noise in an image, 2) produces interferograms with sharp color fringes and 3) prepares the interferogram for phase unwrapping (NEST software).

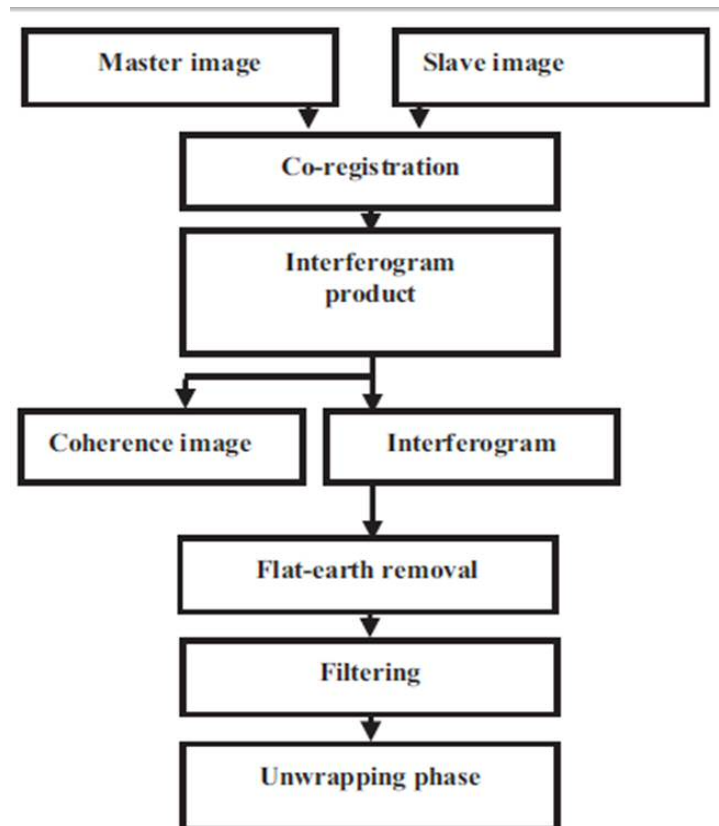


Fig. 2. Interferometry process.

The final products of the interferometric processing chain are the coherence image and the interferogram. The absolute values of the pixels in the coherence product determine whether the interferogram product will display color fringes that are clearly distinguishable (ESA). On the other hand, the interferogram product requires the input of the co-registered stack. To produce the interferogram, the flat earth phase, or the curved reference surface, that is present when the image was acquired, must be removed from the interferogram. Also, the removal of the topographic phase is necessary. This step requires a Digital Elevation Model (DEM), such as SRTM, to be “radarcoded to the coordinate systems of the master image” (NEST software) and then removed from the interferogram (NEST software).

As mentioned before, initially GMTSAR was considered to be used for this project.

Table 3. Algorithm and codes for 2-pass processing - *p2p_SAT.csh*

| | | |
|--|---|---|
| 1 – preprocess <i>pre_proc.csh</i> | <i>update_PRM.csh</i> <i>ALOS_pre_process.csh</i> <i>ALOS_fbd2fbs.c</i> <i>ALOS_fbs2fbd.c</i> | |
| 2 - align and focus <i>align.csh</i> | <i>sarp.csh</i> <i>ALOS_baseline.c</i> <i>xcorr.c</i> <i>fitoffset.csh</i> | <i>esarp.c</i> <i>trend2d.c</i> |
| 3 – topo_ra <i>dem2topo_ra.csh</i> | <i>grd2xyz.c</i> <i>ALOS_llt2rat.c</i> <i>blockmedian.c</i> <i>surface.c</i> <i>topo2phase.c</i> <i>grdimage.c</i> | |
| 4 – interfere and filter <i>intf.csh</i> <i>filter.csh</i> | <i>ALOS_baseline.c</i> <i>phasediff.c</i> <i>conv.c</i> <i>grdmath.c</i> <i>grdimage.c</i> <i>phasefilt.c</i> | |
| 5 – unwrap phase <i>snaphu.csh</i> | <i>grdcut.c</i> <i>grdmath.c</i> <i>grd2xyz.c</i> <i>snaphu.c</i> <i>xyz2grd.c</i> <i>grdimage.c</i> | |
| 6 – geocode <i>geocode.csh</i> | <i>grdmath.c</i> <i>proj_ra2ll.csh</i> <i>grd2kml.csh</i> | <i>grd2xyz.c</i> <i>gmtconvert.c</i> <i>blockmedian.c</i> <i>surface.c</i> <i>grdtrack.c</i> <i>grdimage.c</i> <i>ps2raster.c</i> |

GMTSAR commands are italic. *black* – c-shell script, *red* – GMTSAR C-code, *blue* – GMT C-code, *green* *snaphu* phase unwrapper [Chen and Zebker 2000].

Note this example if for processing an *ALOS* interferogram. For another satellite (e.g. Envisat) replace the characters *ALOS* by *ENVI*.

Results

As mentioned in the introduction of this paper, Remote Sensing Software Graz was used for this project in lieu of GMTSAR. Applying the method of Persistent Scatter InSAR produces the diagram below for the stack of 22 images. The master image of November 28, 2007 is chosen as the master image. As the master image, its orthogonal baseline is set to 0 meters and its temporal baseline is set to 0 days. All other images are stacked after the master image and are set for processing.

The blue lines represent the change in time (or delta time) between image acquisitions. The 21 arcs are shown from the overall master to the other 21 images. An ideal critical orthogonal (or perpendicular) baseline for analysis is less than 1000 meters. But, unfortunately the challenge face in this research were the very large baselines. Many of the baselines (also highlighted in the data table on page three) were more than 1000 meters. These large baselines can lead to increased baseline decorrelations. Furthermore, the blue lines also represent the temporal baseline of the images which was also larger than the repeat cycle of the 46 days for ALOS PALSAR to acquire images.

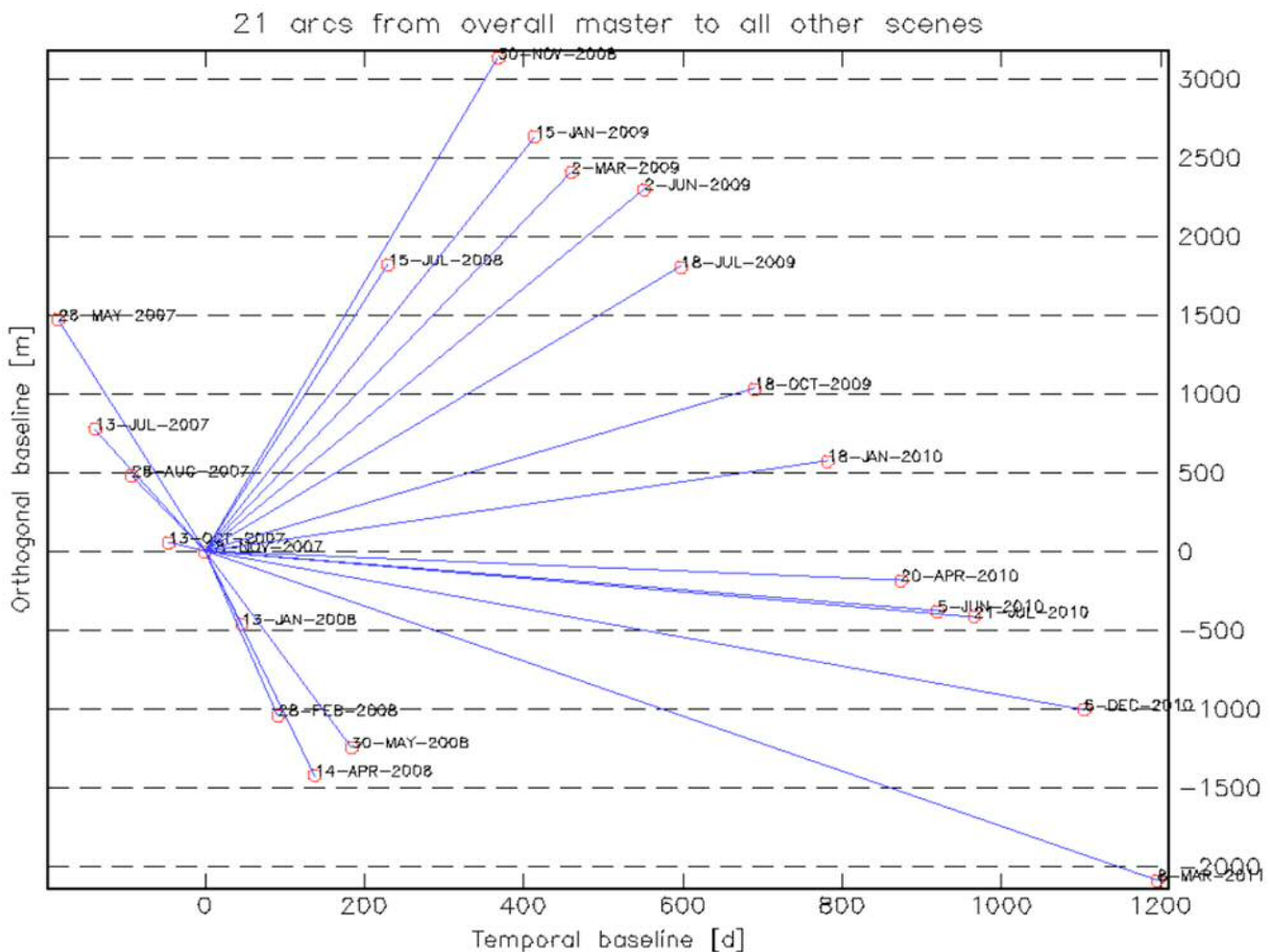


Diagram 1: 21 arcs from overall master and slave images.

In the second diagram below, the a combination of larger and smaller baseline are shown. larger baselines are emphasized. By applying the stacking method via the short baseline subset approach in the Persistent Scatter Method. As a result, a total of 56 interferograms were produced in the process using the Remote Sensing Software Graz.

Images with shorter baselines are the best images for analysis such as the dates between March 2, 2009 and June 2, 2009. The master image remains the same as the image at the top of stack of slave images.

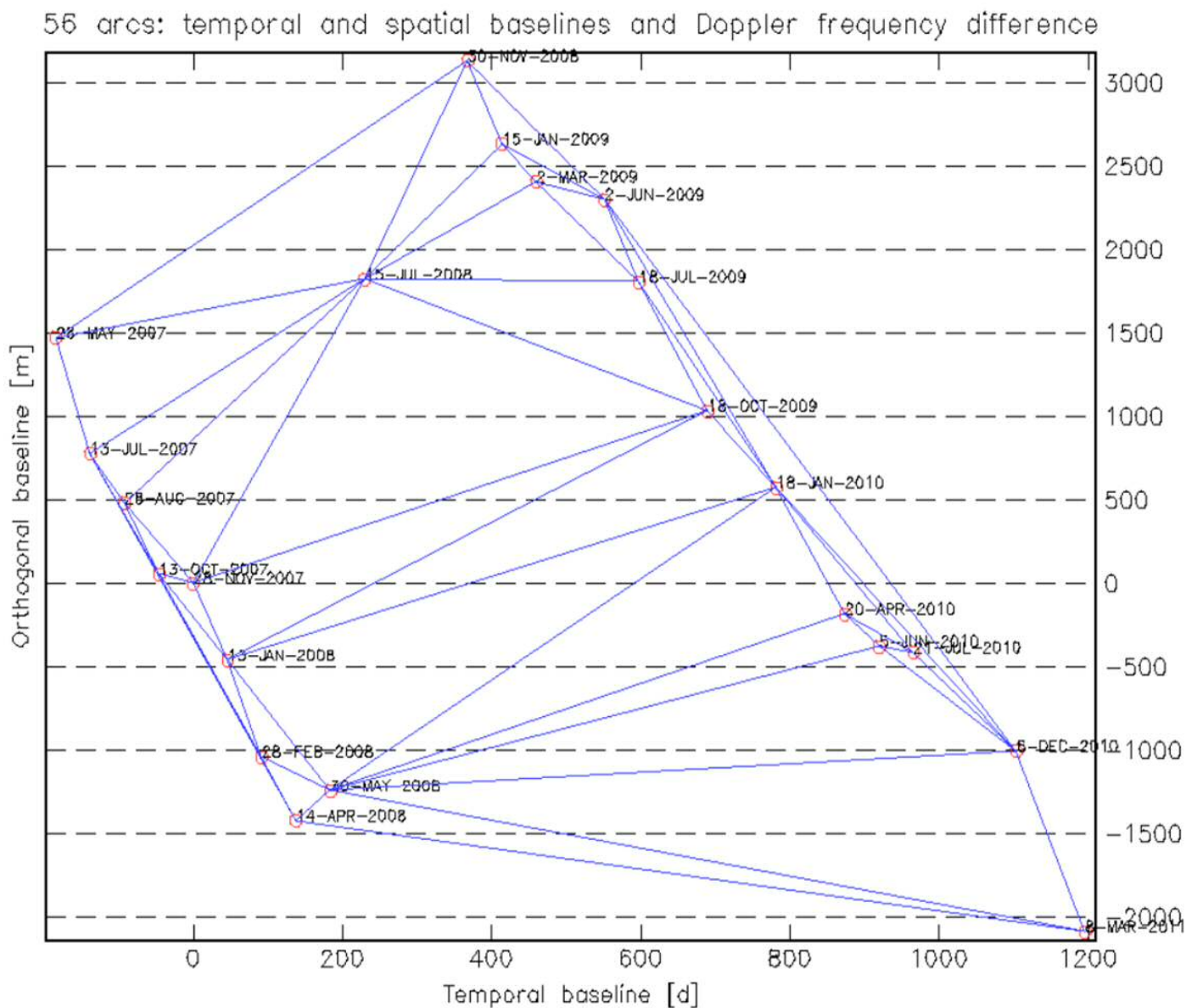


Diagram 2: Perpendicular and Temporal Baselines of all 56 arc interferograms.

Finally, the third diagram below shows the coherence for the stack of interferograms. The diagram shows that the interferograms have very high coherence values in the 0.40 to 0.50 range. This signifies that the signal reflected back to the sensor of the ALOS PALSAR antenna is very strong and therefore, the interferograms will show clear color fringes that display surface displacements on the Earth's surface.

In Diagram three, there are very few interferograms with small coherence values. Therefore, the brighter the coherence image, the better the interferogram. Stack coherence is a very important part of the process of the Persistent Scatter Interferometric Synthetic Aperture Radar in the fact that these images can also display clear indicators of temporal decorrelation or atmospheric anomalies.

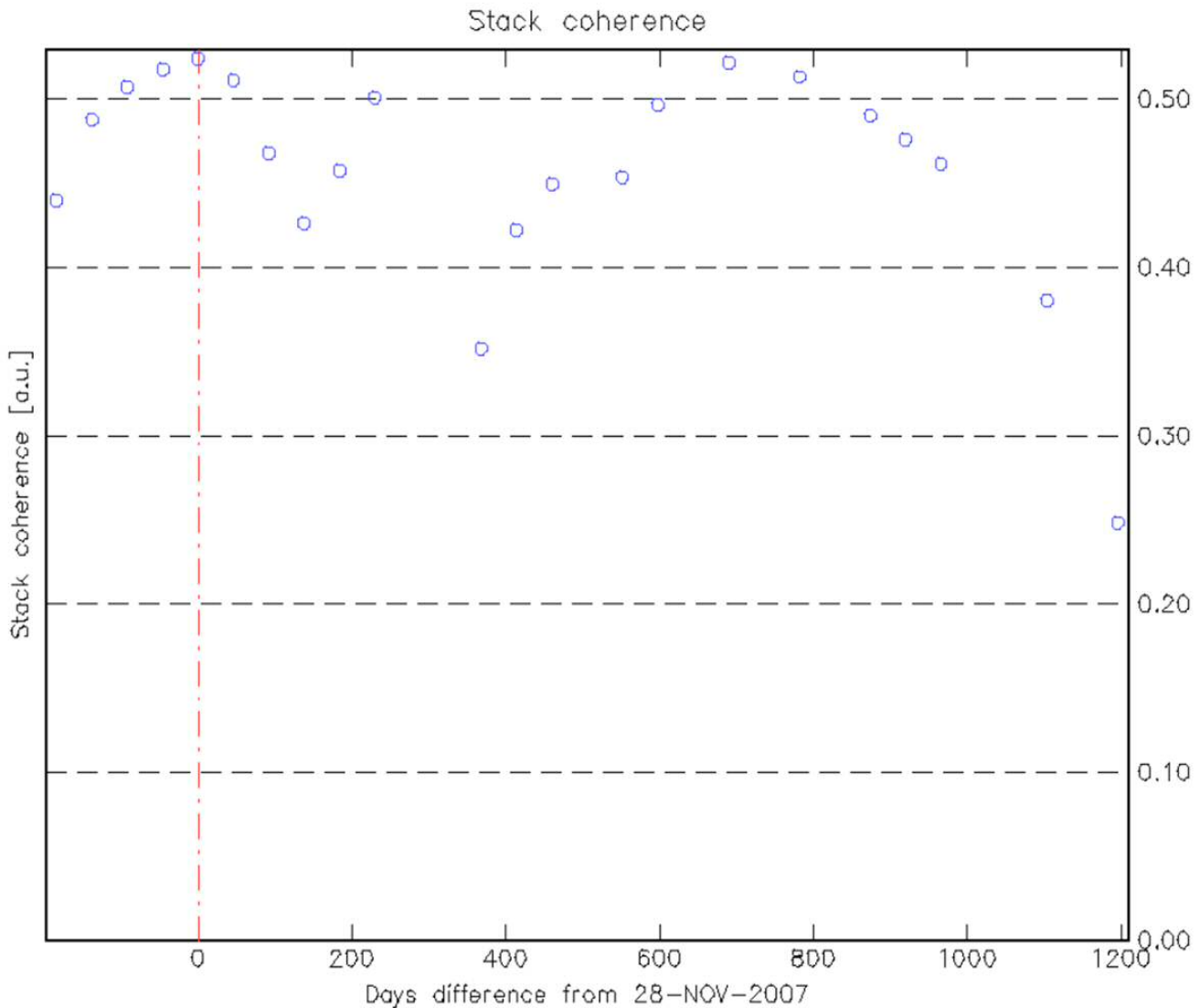
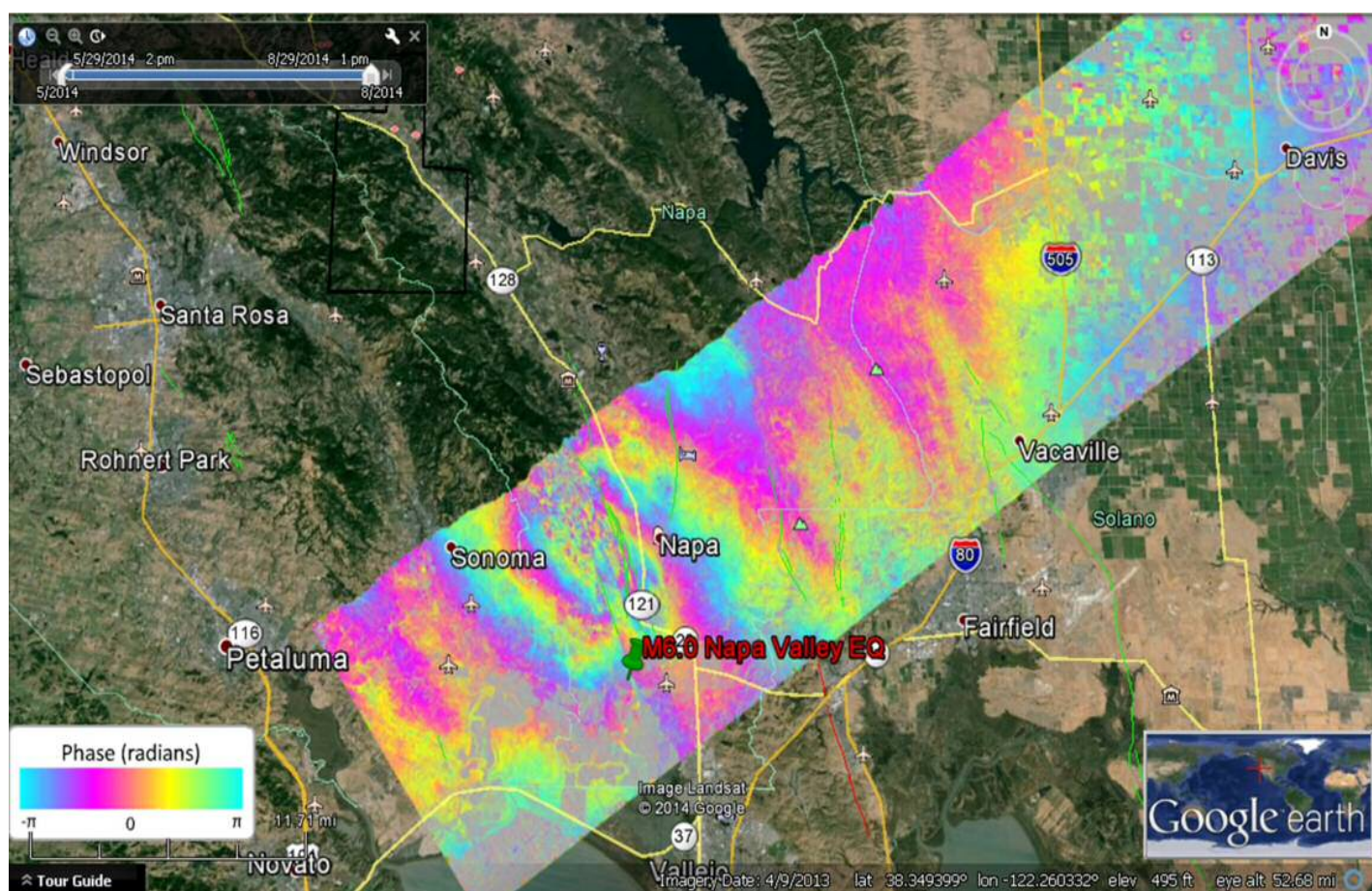


Diagram 3: Coherence of the stack of interferograms.

For the image below, the satellite data was acquired by the National Aeronautical and Space Agency (NASA) via the Unmanned Aerial Vehicle Synthetic Aperture Radar (UAVSAR) mission at the Jet Propulsion Laboratory. The rupture in the middle of the image displays the August 2014 magnitude 6 Napa Valley Earthquake in the Southern Napa Valley Region of California (UAVSAR of NASA/JPL).

The surrounding geography of the area indicates clear fault lines and that this is a highly seismic region given the San Andreas Fault Zone to the West of the rupture. This area is also very mountainous with Sierra Nevada Mountain Range running through the Hayward Rodgers and West Napa Fault Zones. As mentioned in the introduction of this paper, the earthquake struck this region which has experienced low seismic activity (USGS). However, this image is a perfect example of an interferogram with a strong signal reflected back to the synthetic aperture radar sensor on the satellite. The color fringes are clearly shown and are located very close together because of the strong deformation on the surface (refer to “Reading an Interferogram” figure in introduction).

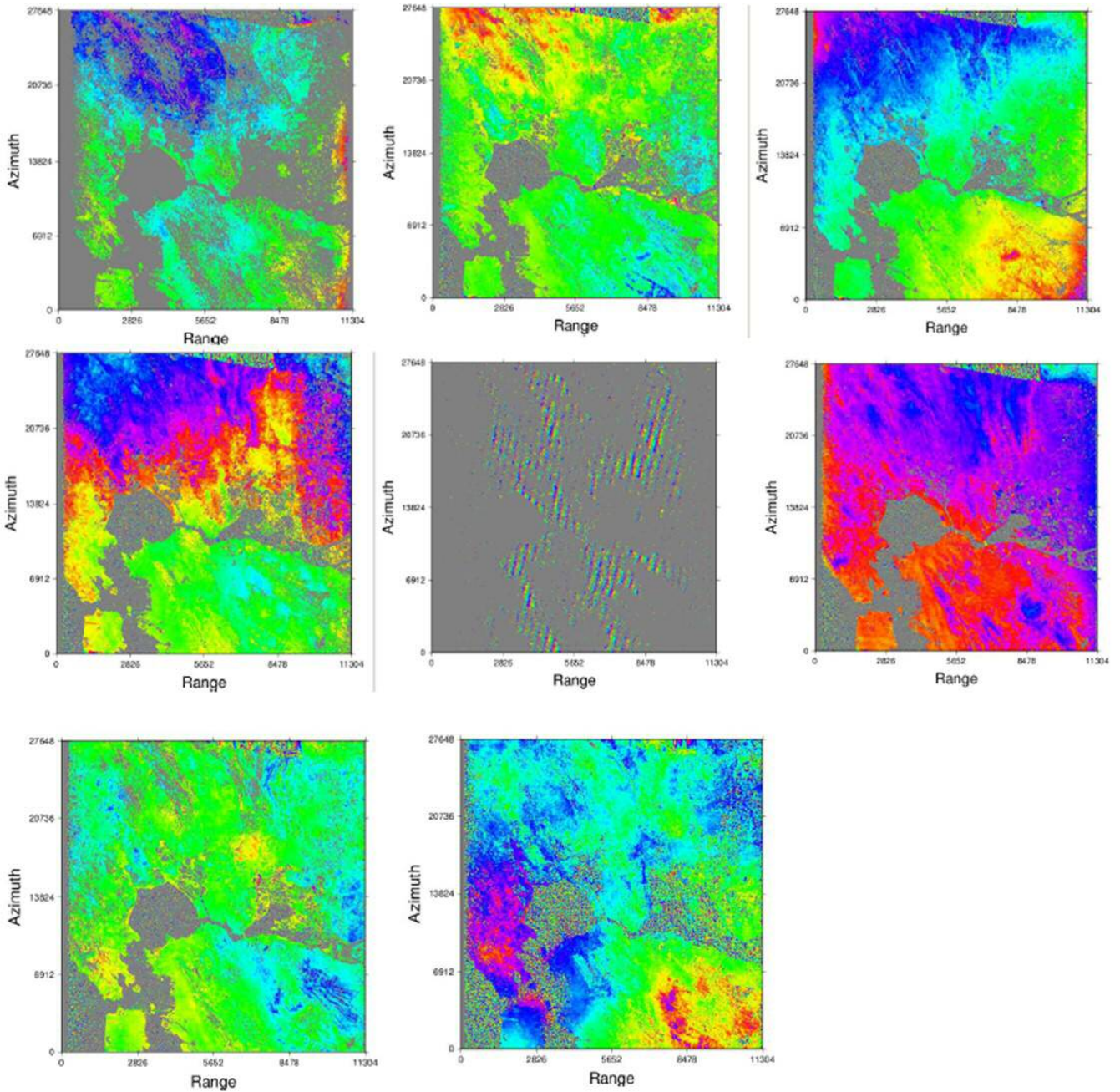


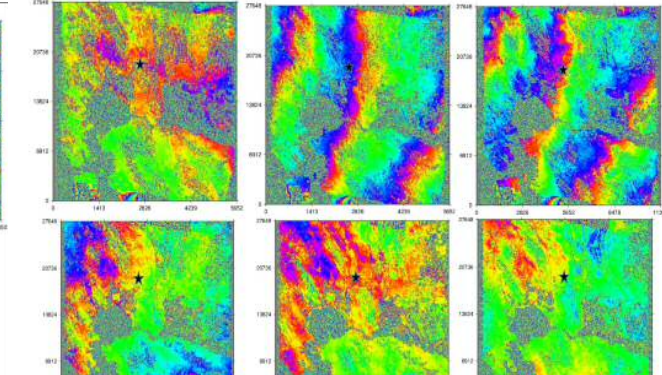
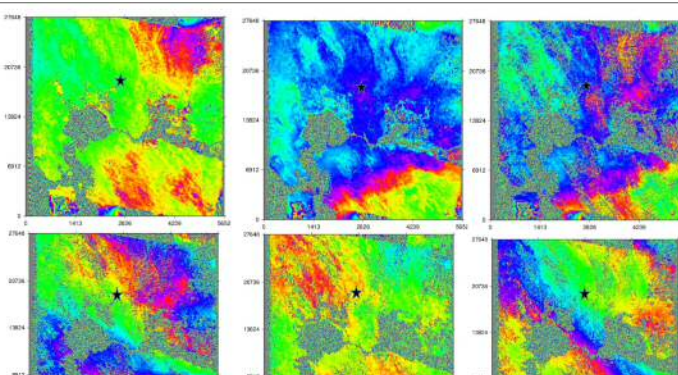
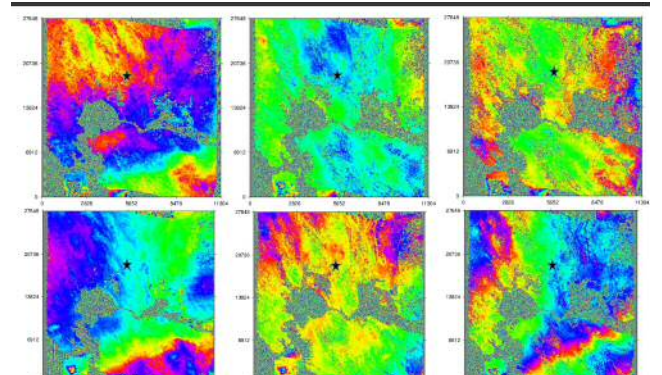
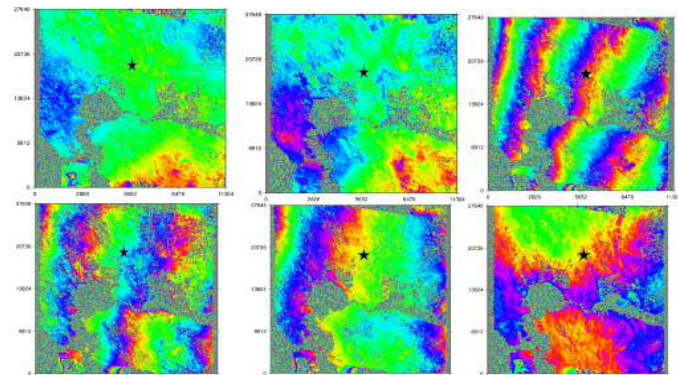
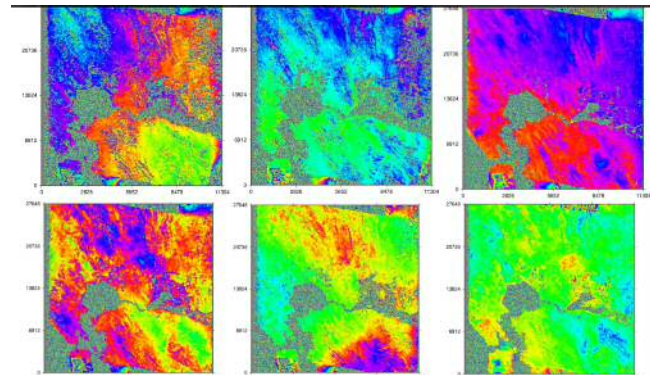
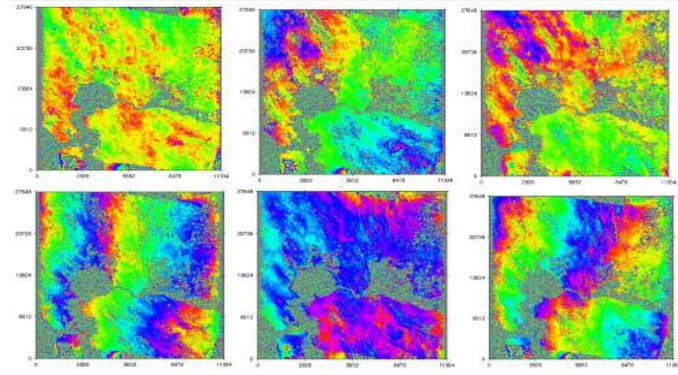
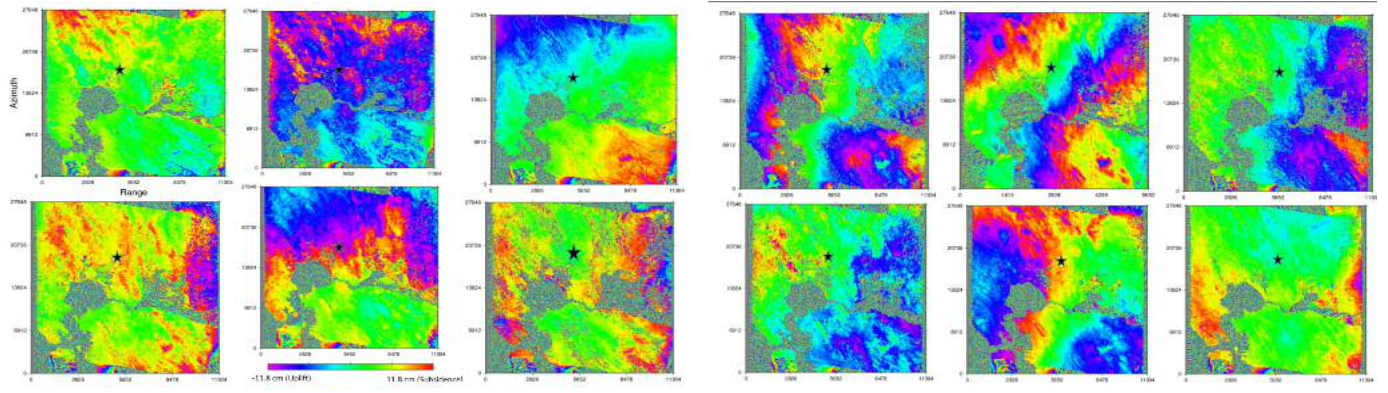
Processed on September 26, 2014 using the Repeat Pass Method in Polarization Mode: HH Polsar acquisition mode on L Band (Flight ID: 14068-001) – Interferogram [Quaternary Faults in Green] (Source: UAVSAR of NASA/JPL)

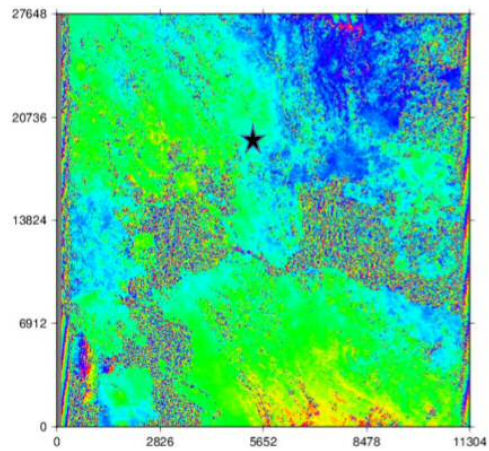
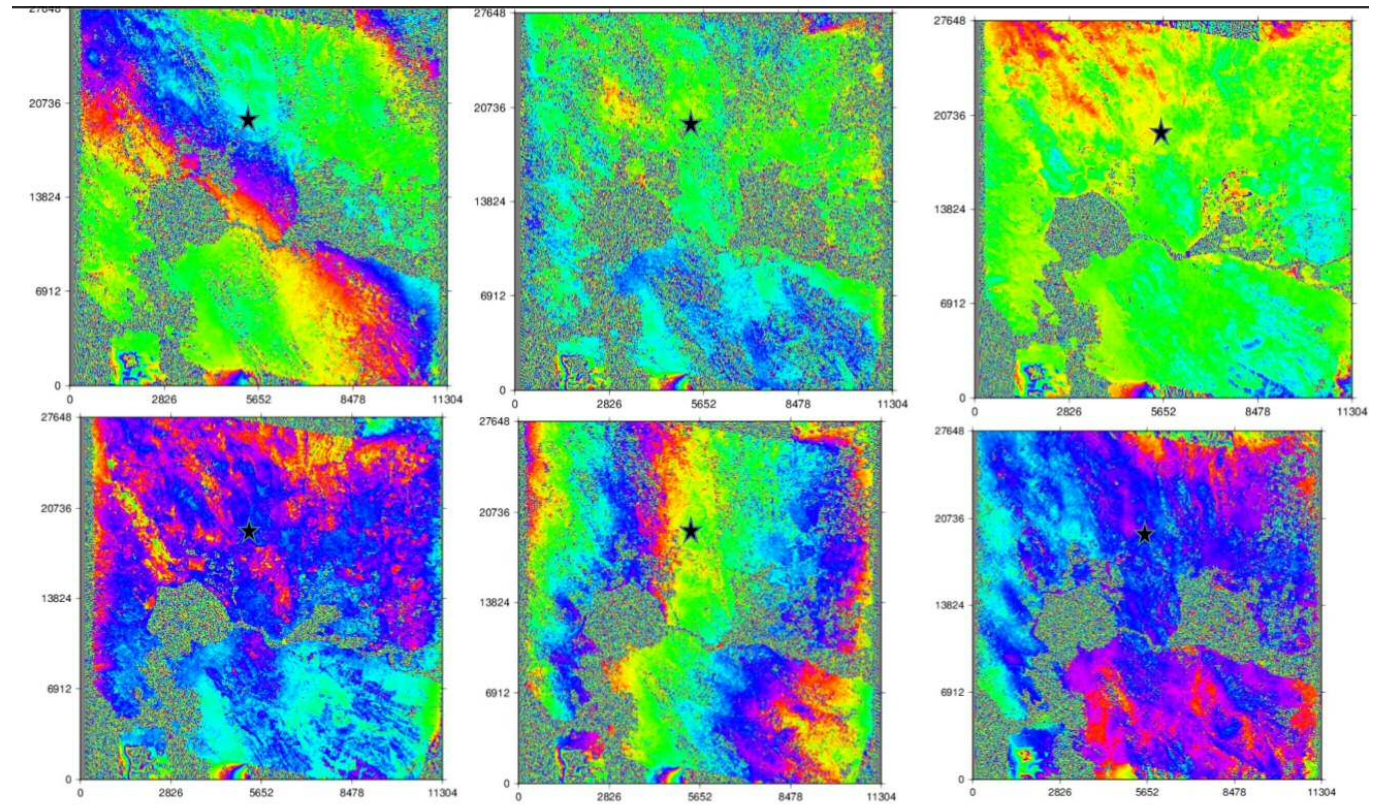
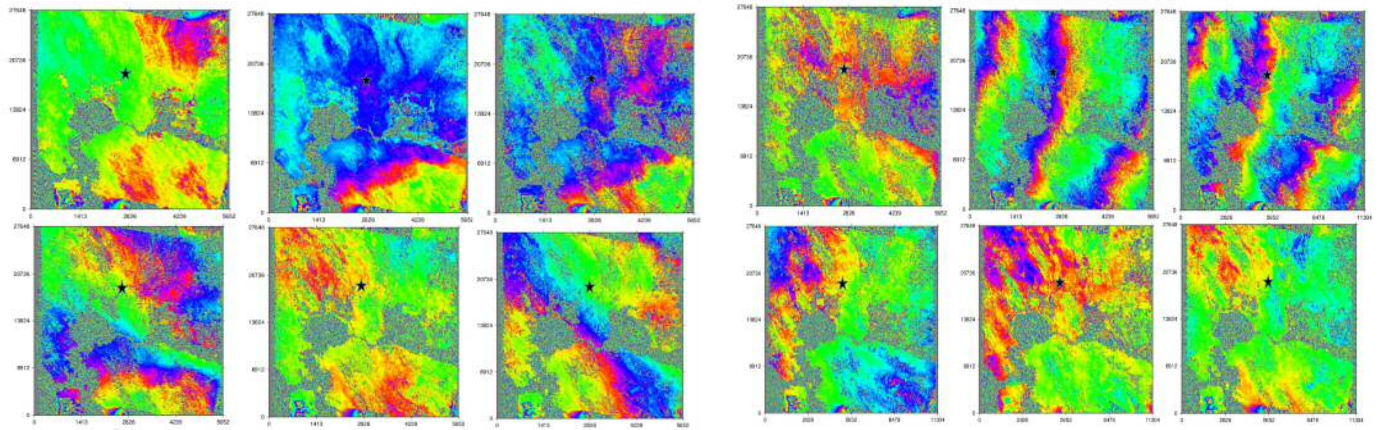
Inteferograms produced by Generic Mapping Tools software



(1 fringe = 11.8 cm displacement (or range change) in LOS (or away from the radar))



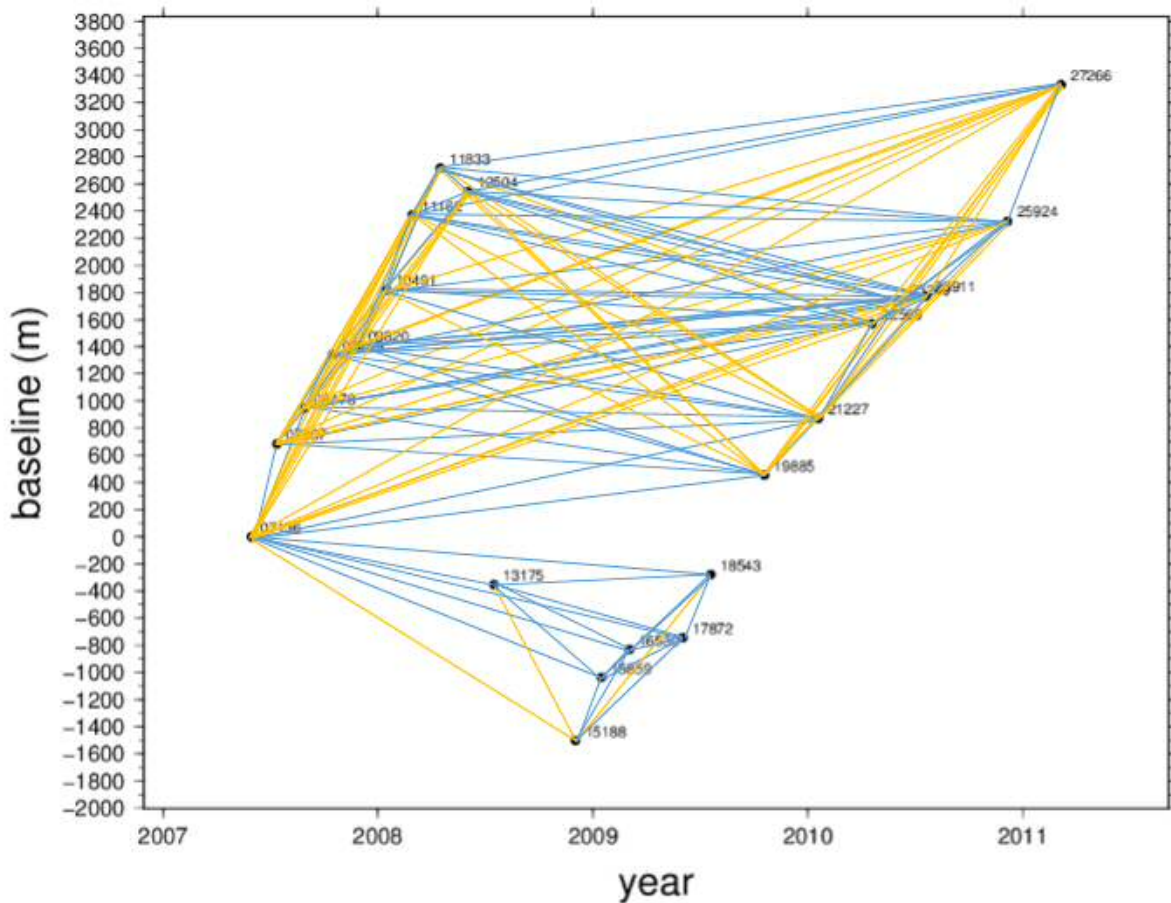




The problems encountered with the interferograms produced with Generic Mapping Tools Synthetic Aperture Radar were vast.

It was anticipated that an InSAR time-series analysis using the interferograms generated across the time span would be a great asset for spatial and temporal detection of surface deformation. But there, were just too many error in terms of the percentage of aseismic deformation and atmospheric effects. Hopefully, the removal of errors approach can contribute to the possibility of establishing an earthquake warning system for the future and strengthening emergency management and evacuation procedures for communities located within the Hayward Fault zone. Potential additional research for this project with GMTSAR include GPS velocity models to track crustal motion near the epicentral region. GPS measurements are compatible with InSAR because GPS measures crustal movement in millimeters per year and acquires “ground-truth” data to cover for satellite data that may be skewed due to errors. Furthermore, acquiring land surface temperature (LST) data using NOAA-AVHRR, MODIS or LANDSAT satellites and using split channel or split window algorithms to detect precursory LST anomalies associated with the Napa earthquake may be beneficial for future research.

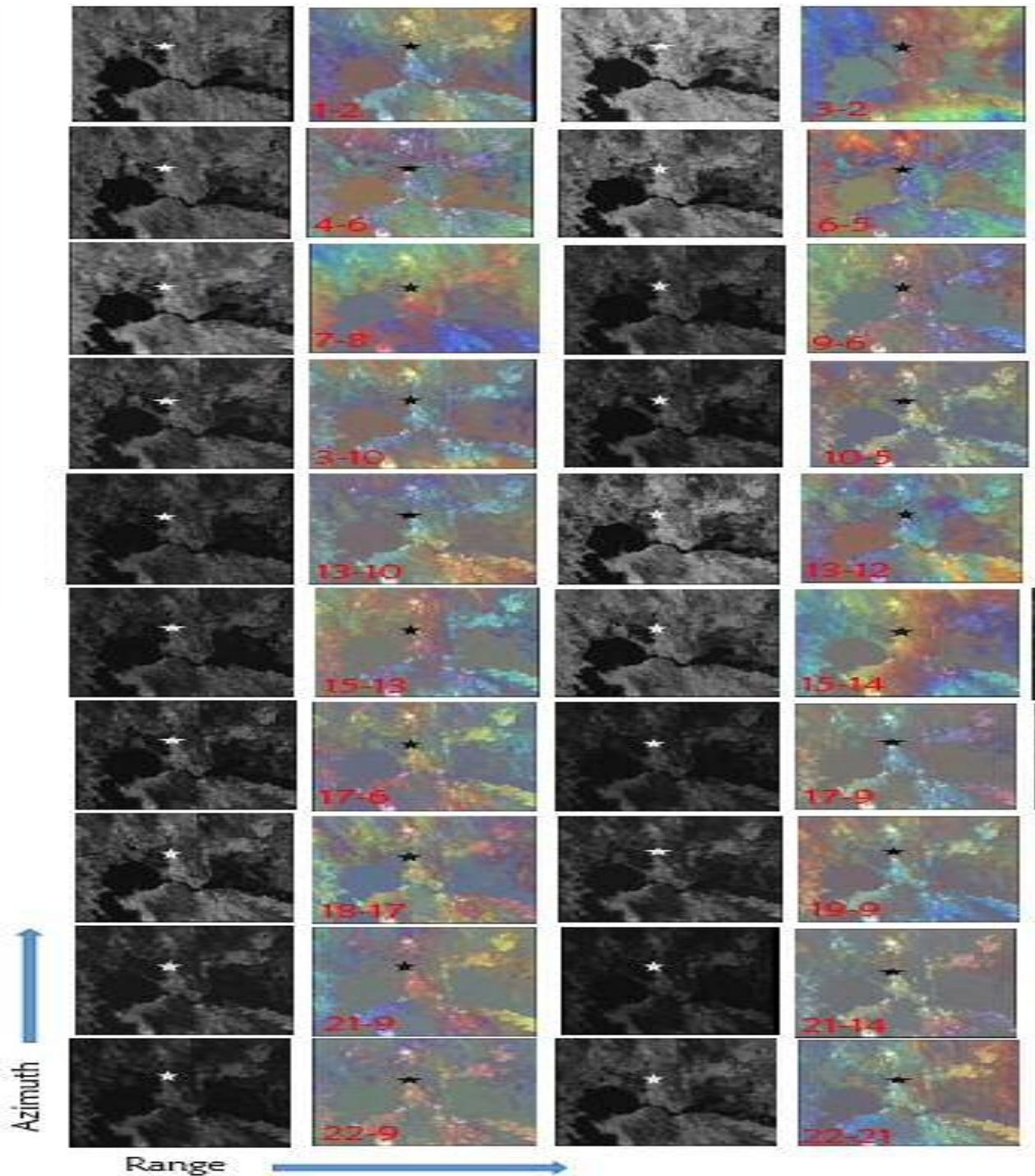
The diagram below also shows massive baselines that cause errors in images

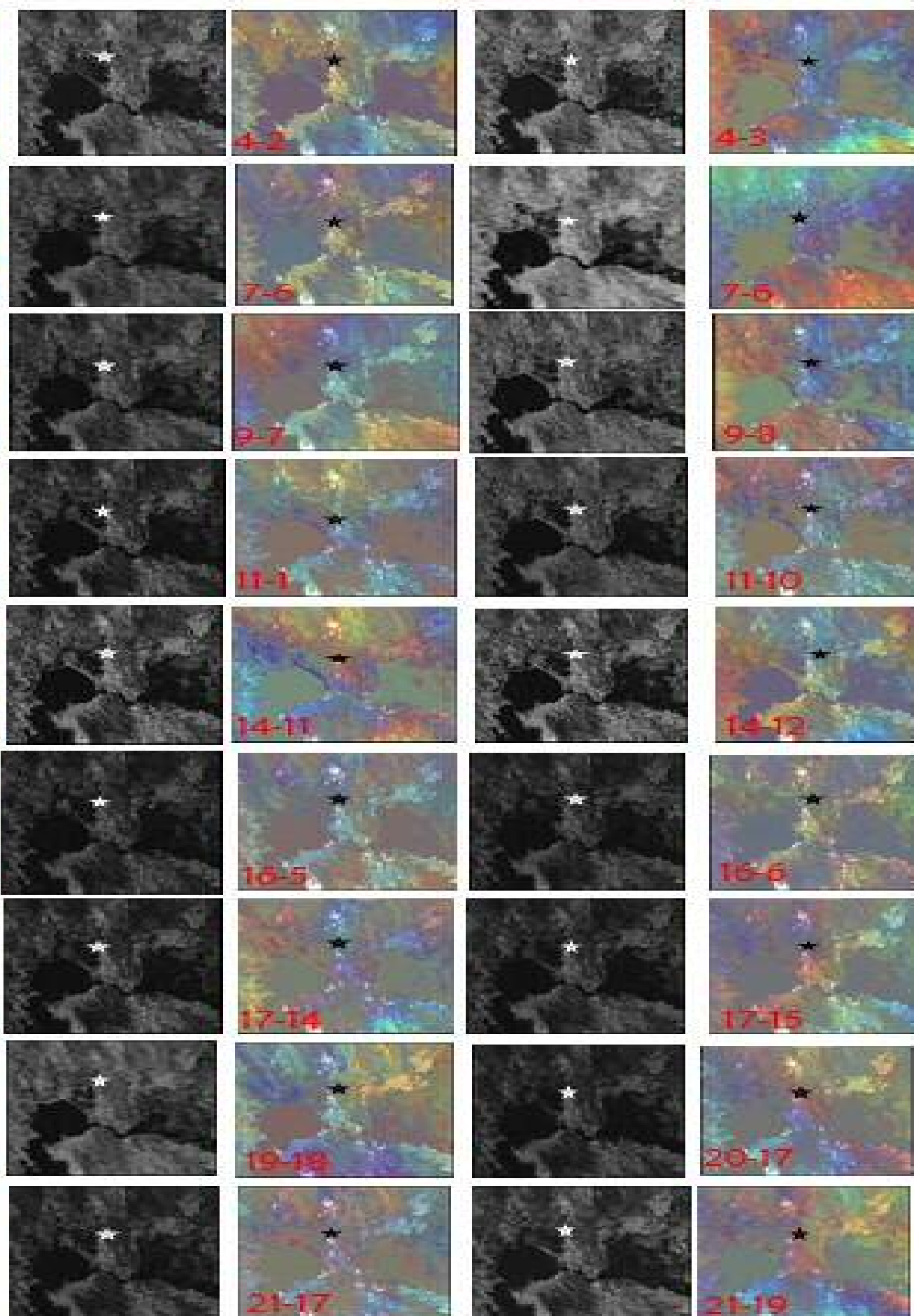


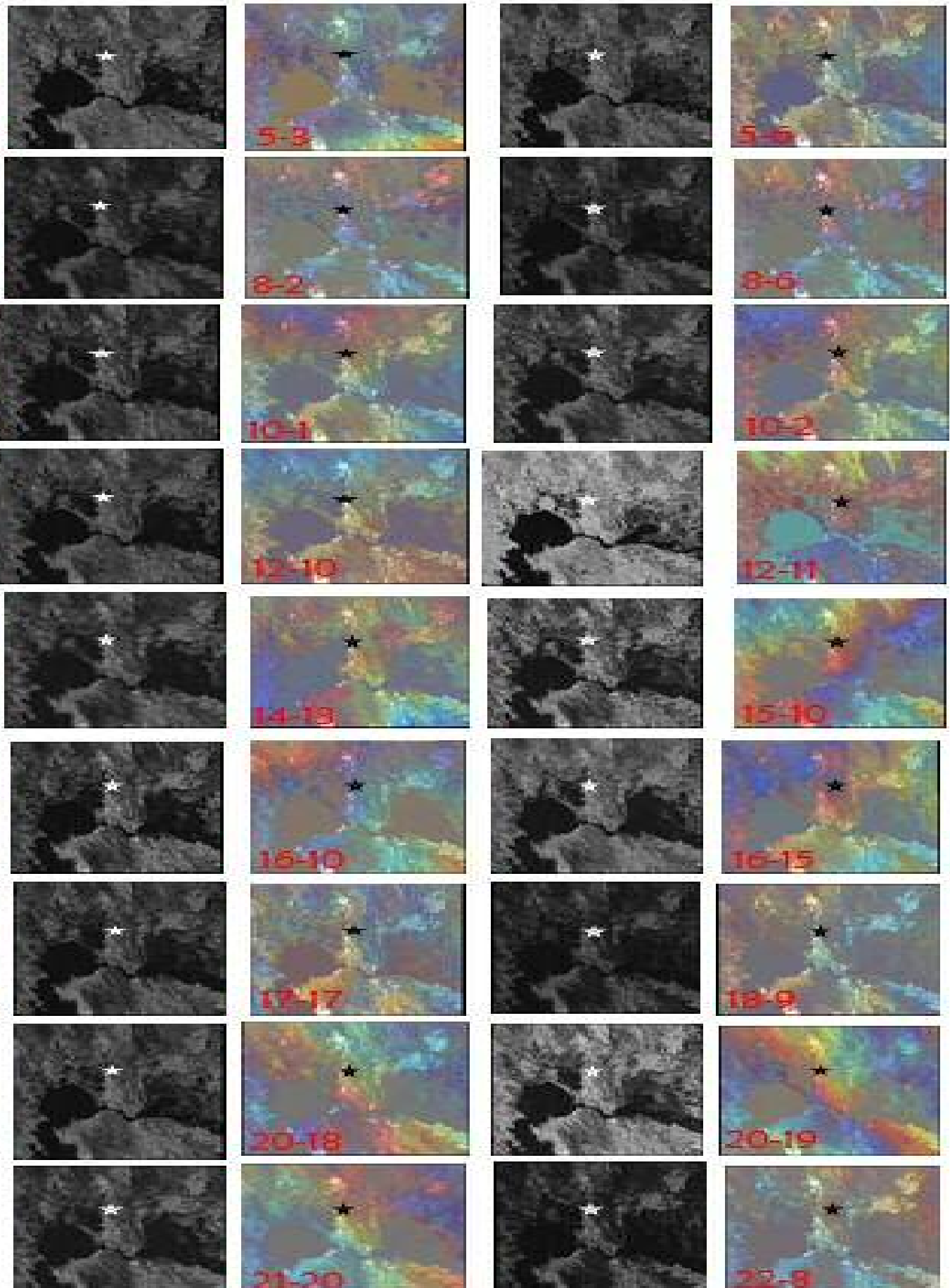
Inteferograms produced by Remote Sensing Software Graz



(1 fringe = 11.8 cm displacement (or range change) in LOS (or away from the radar))







Conclusion

A total of 56 interferograms were produced in this time series data set produced by the Remote Sensing Graz Software. No significant deformation was detected prior to the August 2016 magnitude 6 event. The changes in within each image are likely related to seasonal changes in the water table (no more than 1-3 centimeters of gentle changes). High coherence images reveal good signal strength reflected from the ground. Consistency in data acquisition overall was a challenge in this project.

Furthermore, as previously mentioned, temporal decorrelation and atmospheric anomaly effects were an issue. Moving forward, the biggest challenge we face is with establishing a consistent and reliable warning system that depends on an accurate prediction time frame that includes: 1) establishing an estimated time frame prior to rupture by determining the time between the observation of the deformation and the time or day of the event, 2) determining whether the deformation is tectonic or non-tectonic in origin, 3) observing actively deforming regions with high seismic activity and 4) integrating Global Positioning Satellite (GPS) data with Interferometric Synthetic Aperture Radar data.

Acknowledgements

Special thanks to 1) Dr. Schardt & Dr. Gutjahr at the Joanneum Institute for the advisement & software, 2) Dr. Brathwaite, NYC-LSAMP/NSF & the Austrian Marshall Plan Foundation for awarding me the scholarship & providing funding, & 3) support from my family & fellow LSAMP peers.

References

Chelbi, S., Khireddine, A., Charles, J.P. Interferometry process for satellite images SAR. *International Conference on Electrical and Electronics Engineering*. 2011. 180-184.

RSG, 1993, Remote Sensing Software Package Graz. Software User Manual, 3rd edn, Institute for Digital Image Processing, JOANNEUM RESEARCH, Graz, Austria.

Japan Aerospace Exploration Agency (JAXA)

United States of America Geological Survey (USGS) http://earthquake.usgs.gov/earthquakes/eventpage/nc72282711#impact_shakemap.

Japan Aerospace Exploration Agency (JAXA) and Sentinel 1 (ESA).

Sandwell et al. Generic Mapping Tools Synthetic Aperture Radar Manuel. University of California San Diego 2011.

Ouchi, Kazuo. Recent Trench and Advance of Synthetic Aperture Radar with selected topics. *Remote Sensing*. 2013. 5(2): 716-807.